ACTIVE REDUCTION OF HIGH-LEVEL ACOUSTIC NOISE ON A FMRI TEST-BED USING LABVIEW AND FPGA PLATFORMS

Venkat R. Ramachandran [(1)], Issa M. S. Panahi [(1)†], Eduardo Perez [(2)].

[(1)]The University of Texas at Dallas, Richardson, USA, [(2)] National Instruments Inc, Austin, USA.

ABSTRACT

We present an Active Noise Control (ANC) system that is designed to cancel acoustic noise at high sound levels. The ANC system is graphically designed using LabVIEW and implemented on FPGA. NLMS algorithm is used for updating the filter co-efficients. The ANC system is evaluated on a realistic test-bed mimicking an actual fMRI bore. The algorithm is tested for various tonal frequencies in the range from 100 to 5000 Hz and the performance is measured in terms of the noise cancellation. We observe that good noise cancellation (15 to 45 dB SPL) can be obtained with NLMS algorithm over the entire bandwidth.

Index Terms— Real time ANC, LabVIEW, FPGA, NLMS.

1. INTRODUCTION

In high magnetic field (3 Tesla and higher) fMRI scanners, the acoustic noise produced during scans reaches over 130 dB Sound Pressure Level (SPL) [1],[2]. Such loud acoustic noise is not only harmful to the patient undergoing the MRI scan but also a major interference to the audio communication often needed to and from the patient. The scanner noise may activate spurious areas of the auditory cortex affecting fMRI experiments in which it is desired to stimulate the auditory regions of the brain. This reduces the dynamic range available for activation by the stimulus of interest. The reduction of acoustic noise during scanning is of great interest for conducting advanced fMRI experiments.

Passive active noise control methods such as ear-muffs and ear-plugs can be used to partially reduce the noise heard by the patient. However, they are ineffective for low frequencies. A solution to the problem is Active Noise Control (ANC) where the acoustic noise is actively cancelled by equal magnitude and opposite phase signal. Reducing the acoustic noise and achieving a zone of silence around the patient's head using ANC systems is of research interest [3]. The noise reduction improves the patient's comfort level and enhances the audio communication between the patient and the researcher. This paper discusses the real-time implementation of a LMS-based ANC system on a realistic test-bed mimicking an actual fMRI bore and setup. There are several papers that deal with noise cancellation experiments conducted in a narrow acoustic duct. However, the dimensions of the duct are small and the noise control can be characterized as a one-dimensional problem. Our work differs in that the ANC system is implemented and tested on realistic half-cylinder cavity of the size of an actual fMRI bore. So, the noise control is characterized as a more complex three-dimensional problem.

The ANC system includes a PC running on a Real-time Operating System (OS) and a PCI card, 7833R, which embeds ADC and DAC units. An on-board user reconfigurable Input/Output FPGA (with 3M gates) controls the functionality and timing of 7833R. LabVIEW 8.2, as a graphical design tool, and associated software are used to program the device operating in 16-bit fixed point high-speed state machine. The system is tested with several sine tones of frequencies between 100 and 5000 Hz on the test-bed. The design achieves high speed sampling loop necessary for minimizing computational delay and satisfactory operation of the ANC adaptive algorithm. The performance of the algorithm is evaluated under high sound levels (90 – 115 dB SPL).

The organization of the paper is as follows: Section II discusses the adaptive algorithm used for updating the filter co-efficients. Section III describes the experimental setup and the hardware design. Sections IV and V describe the secondary path estimation method, and the LabVIEW programming and FPGA design, respectively. The results of the experiments are discussed in Section VI.

2. FXNLMS ALGORITHM

The block diagram of an ANC system is shown in Fig.1. *d(n)* refers to the acoustic signal that has to be cancelled.

† Supported by a subcontract from the Epidemiology Division, Department of Internal Medicine, U.T.Southwestern Medical Center at Dallas under grant no. DAMD17-01-1-0741 from the U.S. Army Medical Research and Materiel Command. The content of this paper does not necessarily reflect the position or the policy of the U.S. government, and no official endorsement should be inferred.

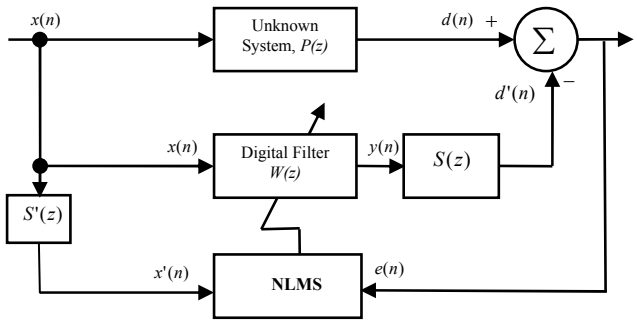

Fig.1. Block diagram of a ANC system that uses NLMS algorithm. The adaptive filter *W(z)* tries to cancel *d(n)* by estimating it from *x(n)*. *d'(n)* is the filter estimate of *d(n)*. *e(n) = d(n) – d'(n)*.

The adaptive filter tries to estimate *d(n)* from the reference signal *x(n)* and the error signal. *d'(n)* is the estimate of *d(n)*. The error signal *e(n) = d(n) – d'(n)*) is fed back to the algorithm. The objective of the ANC system is to minimize *e(n)*. An ANC system differs from the traditional system identification scheme in the use of an acoustic summing junction instead of the subtraction of electrical signals. *S(z)* refers to the (microphones, loudspeaker, electrical and acoustic paths) transfer function between the output of the adaptive filter to the point where the error signal gets recorded. *S'(z)* is an estimate of *S(z)*. The estimation and significance of the secondary path transfer function is discussed in Section IV.

Filtered-x Normalized LMS (FXNLMS) algorithm is used for updating the filter co-efficients. The weight updating case of the FXNLMS algorithm is as follows.

$$\mathbf{x'}(n) = \mathbf{x}(n) * s'(n)$$

$$\mathbf{w}(n+1) = \mathbf{w}(n) + \frac{\mu\, e(n)\mathbf{x'}(n)}{\sum_{i=1}^{N} \mathbf{x'}^2(n-i+1)} \qquad (1)$$

where, n is the sample time index, μ is the step size $0 < \mu < 2$, N is the adaptive filter length, * denotes convolution, $e(n)$ is the error signal where $e(n) = d(n) - [\mathbf{w}^T(n)\mathbf{x}(n)]$, $s'(n)$ is the impulse response of the estimated secondary path *S'(z)*, $\mathbf{w}(n) = [w(n), w(n-1), ...w(n-N+1)]^T$ defines the co-efficients of the ANC cancelling FIR filter $W(z)$ and $\mathbf{x}(n) = [x(n), x(n-1), ..., x(n-N+1)]^T$ represents N samples of the input or reference data. Detailed discussion about FXNLMS algorithm can be found in [4].

3. LABORATORY SETUP AND HARDWARE

The block diagram of the experimental setup is shown in Fig.2. A half cylinder made of transparent acrylic (thickness 2.5 cm) mounted on a plywood base (thickness 2.5 cm) was used in all our experiments to mimic actual acoustic cavity of the fMRI bore. The dimensions of the structure are

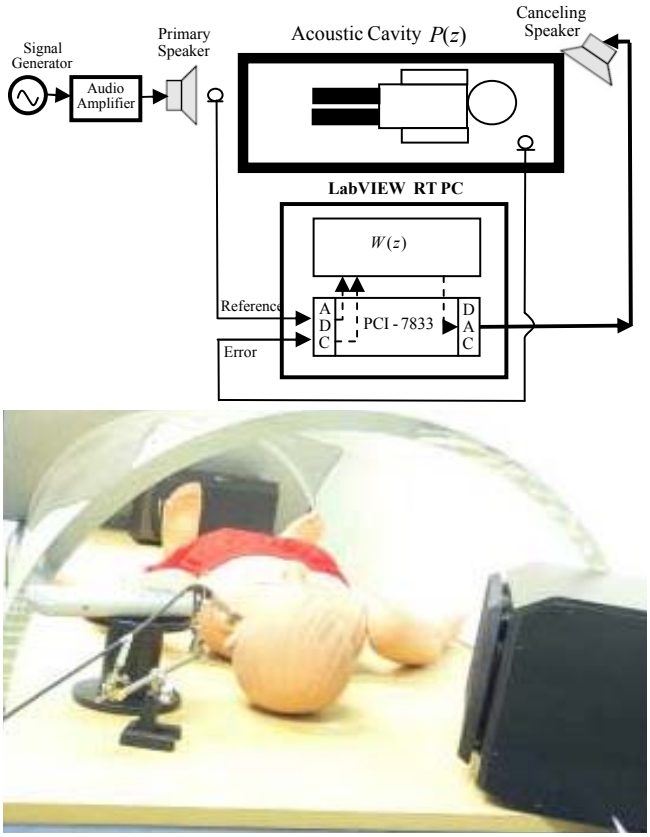

Fig.2. Block diagram and photograph of the laboratory experimental setup. Primary loudspeaker is placed on the one end of the bore. Reference microphone is placed close to the primary speaker. Canceling loudspeaker is placed on the other end of the bore, close to the head of the manikin. Error microphone is placed close to the ear of the manikin. SPL meter measures the error sound level.

length; 1.5 m (5 feet), and diameter; 0.76 m (2.5 feet). The laboratory room dimensions are 4.5 m × 2.8 m × 2.6 m (H).

A full-size manikin is placed inside the bore to imitate a human body. The primary source of acoustic noise was generated using an 8 ohm impedance loudspeaker (placed in one end of the bore). A function generator / PC sound card generates the noise signal which is amplified by an audio amplifier and sent to the loudspeaker. The frequency response of the primary loudspeaker ranges from 55 Hz to 22 kHz with a maximum power output of 125 W. The canceling loudspeaker has similar specifications as the primary loudspeaker and is placed on the other end of the bore. The anti-noise output is also amplified by the audio amplifier and sent to the canceling loudspeaker. The audio amplifier has 4 channels with a 20 Hz – 20 KHz frequency bandwidth and a maximum average output power of 200Watts per channel.

Two diffuse-field microphones (designed to have omnidirectional response and a large dynamic range) are used to acquire the reference and error signals. The reference microphone is placed behind the primary

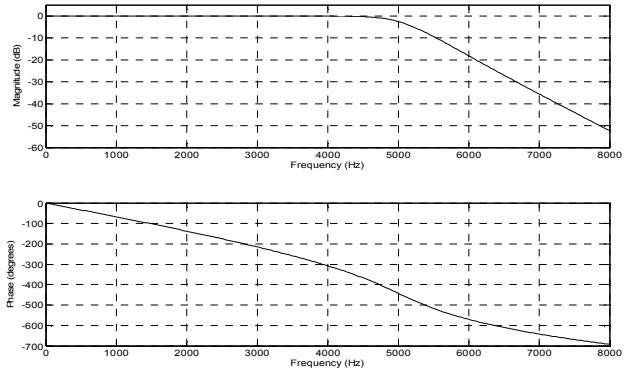

Fig.3. Frequency response of the 10th order analog Butterworth filter, F_C = 5000 Hz.

loudspeaker and covered with foam to avoid feedback from the canceling loudspeaker. The error microphone is placed close to the ear of the manikin. The ANC system processes the signals to determine the anti-noise. The ANC system consists of (1) Real-Time (RT) Target and (2) PCI 7833R.

RT target is a Pentium-IV 1.8 GHz PC. The RT target has an Intel 82550 Ethernet chipset mounted on its PCI chassis. National Instruments PCI 7833R is a multi-function Data acquisition (DAQ) device that has 8 analog inputs and 8 analog outputs with a 16-bit (ADC, DAC) resolution and an operating voltage range of ± 10V [5]. It is mounted on the PCI chassis of the RT target. The 7833R board has 3 million reconfigurable gates which can be used to control the analog I/O lines.

In ANC systems, control loop time is very critical. The loop time has to be deterministic with minimum jitter for effective noise cancellation. Windows OS cannot ensure that the code will execute within certain time limit and is generally not used for real-time applications. Applications requiring extended run times or stand alone operation are often implemented with Real Time OS. The RT target runs on the real-time operating system of Venturcom – Phar Lap Embedded Tool Suite (ETS) [6].

The RT target acquires the input signals from 7833R, processes it and generates the anti-noise signal which is then amplified and sent to the canceling loudspeaker. A 10th order analog Butterworth Low Pass filter with a cut-off of 5 kHz is used to smoothen the analog output of 7833R. The frequency response of the filter is shown in Fig.3.

4. SECONDARY PATH ESTIMATION

The secondary path transfer function *S(z)* includes the Digital to Analog (D/A) converter, reconstruction filter, power filter, loudspeaker, acoustic path from the canceling loudspeaker to the error microphone, error microphone, anti aliasing filter, Analog to Digital (A/D) converter, and the acoustic path (air gap) between the loudspeaker and error microphone. The introduction of secondary path transfer function *S(z)* can cause system instability. This is because

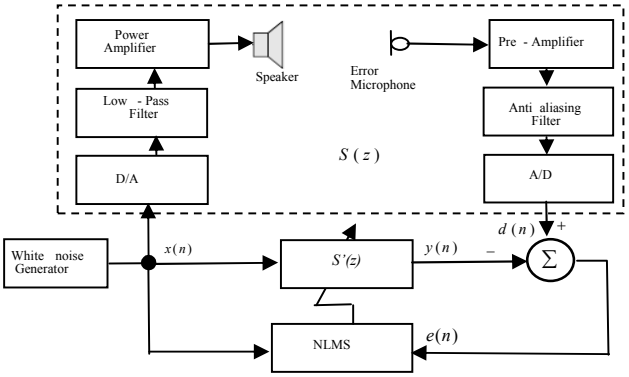

Fig.4. Block diagram of the offline secondary path estimation. White noise is used to train the system.

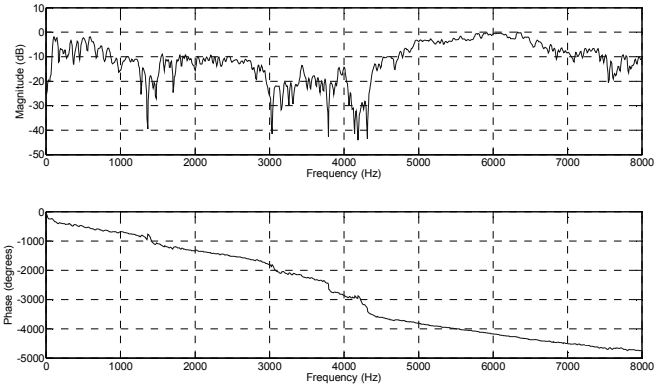

Fig.5. Frequency response of the *S'(z)* – 1024-tap FIR filter. Frequency ranges from 0 – 8000 Hz.

the error signal is not correctly aligned with the reference signal. The solution to this problem is placing a filter identical to *S (z)* in the reference signal path to the NLMS algorithm, as seen in Fig.1. The block diagram to estimate the secondary path is shown in Fig.4. White noise is used to train the system. The transfer function is assumed to be linear and time invariant. It is modeled offline and the estimate, *S'(z),* obtained at the end of the training period is used in our experiments. The frequency response of 1024-tap FIR filter *S'(z)* is shown in Fig.5.

5. LABVIEW AND FPGA PROGRAMMING

The ANC system is programmed graphically using LabVIEW 8.2, LabVIEW RT 8.2 and LabVIEW FPGA 8.2. Graphical interface makes the programming simpler and debugging easier. A LabVIEW program/subroutine is called a virtual instrument or VI. Programming of the ANC system consists of two parts:

(1) FPGA VI for programming the 7833R board and,

(2) RT VI for programming the adaptive filter on the RT desktop.

LabVIEW RT module executes VIs on the RT target (running on ETS OS). However, the RT VIs cannot be

programmed on the RT target directly. The RT target communicates with another computer (the host PC) through an Ethernet crossover cable. The host PC runs on Windows and has LabVIEW and LabVIEW RT module installed on it. The VIs are developed on the host PC and downloaded on the RT target.

LabVIEW FPGA 8.2 is used to graphically program 7833R system. The FPGA VI is used to customize the inputs and output channels and also control their timings. The FPGA VI also includes filters to remove the DC offset and 60 Hz electrical noise interference. The input mode in 7833R unit is software configurable. Differential mode is chosen to remove any common mode noise between the two input lines (AI+ and AI−) of the analog input. Our design of the FPGA VI also includes *S'(z)* to filter the reference input. In our design the FPGA was configured for both 16-bit and 32-bit fixed-point representation of data. The FPGA VI is then compiled so that it can be run on the FPGA. The output of the compile process is a bitstream that is downloaded onto the FPGA. During the compile process, LabVIEW converts the VI into intermediate VHDL files which are then passed to the Xilinx compile server. The compile server then compiles the VHDL into the resulting bitstream. The bitstream is then stored in the VI by the LabVIEW environment [7].

On their own, the VIs on the RT target and FPGA VI run asynchronously. Synchronization is required for lossless data transfer between the VIs. Synchronization is achieved between the RT target and 7833R board using the interrupt method. The FPGA VI generates an interrupt when the data is ready. The RT VI uses 'Wait on IRQ' to wait for an interrupt. An acknowledge signal is sent from the RT target to the 7833R unit once the data is received. It is noted that the FPGA VI acquires data at a rate of 100 kHz (sampling time of 10 µs). However, the RT VI on the RT target works on lower loop rates of 30 – 40 kHz. So, the overall control loop rate of the ANC system ranges between 30 – 40 kHz.

6. RESULTS

The ANC system is tested with several sine tones in the frequency range 100 to 5000 Hz. A SPL meter is placed close to the error microphone to measure sound levels before and after cancellation. A NLMS based FIR adaptive filter (1) of length 16 and step-size of 0.01 was used for our experiments. The RT VI was executed and the noise attenuation levels were noted. Fig.6 shows the initial noise levels (before cancellation), final noise levels (after cancellation) and the amount of noise cancellation for various frequencies.

The fMRI noise data recorded from a 3 Tesla Siemens Magnetom Trio [1] had dominant frequencies at 600 Hz, 1150 Hz and 1600 Hz. The attenuation levels of the single tone signals at those frequencies were 28 dB, 23 dB and 27 dB, respectively.

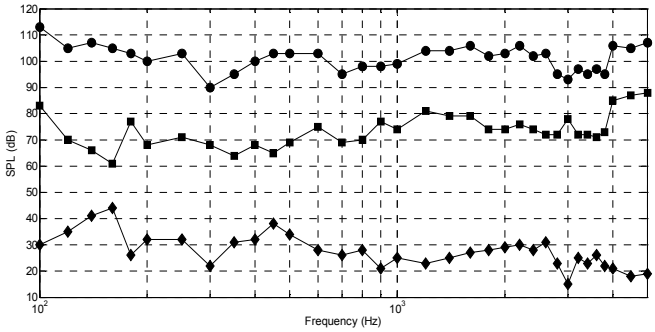

Fig.6. Performance of the ANC system for the frequency range 100 to 5000 Hz. The top-most line (with circles) indicates the initial noise level over the entire bandwidth. The second line (with squares) indicates the noise level after ANC over the entire bandwidth. The lowest line (with diamonds) indicates the amount of noise cancellation over the entire bandwidth. Noise cancellation = initial noise level (circles) – final noise level (squares).

It must be noted that the area of cancellation is proportional to the wavelength of the signal. As the frequency increases, the area of cancellation becomes smaller and the attenuation is restricted to a smaller area around the error microphone (which is placed close to one ear of the manikin). So, the noise will be cancelled in only one ear and would be audible in the other. Multi-channel ANC will be used next to obtain desired noise cancellation in both the ears.

7. CONCLUSION

A LabVIEW based ANC System is implemented and the performance is evaluated using sine tones from 100 to 5000 Hz. High control loop rates between 30 – 40 kHz are achieved. Attenuation levels between 15 to 45 dB SPL are observed over the entire bandwidth. It is noted that the zone of silence decreases with increase in frequency and acoustic noise cancelled in only one ear. This can be overcome by the use of multi-channel ANC.

8. REFERENCES

[1] V. Ramachandran, et al, "Multi-band Speech Enhancement for Functional MRI," *ICASSP* Proceedings, Toulouse, France, May 2006.

[2] M. Ravicz, J. Melcher, et al, "Acoustic Noise during Functional Magnetic Resonance Imaging," *Journal of Acoustic Society of America*, 108(4), October 2000.

[3] M. McJury, et al, "The Use Of Active Noise Control (ANC) to Reduce Acoustic Noise Generated During MRI Scanning: Some Initial Results," Magnetic Resonance Imaging, Vol. 15, No. 3, 1997.

[4] S. M. Kuo and D. R. Morgan, Active Noise Control Systems - Algorithms and DSP Implementations, John Wiley & Sons, Inc. 1996.

[5] National Instruments Inc, Austin, TX, USA, "NI 783xR User Manual", June 2006.

[6] National Instruments Inc, Austin, TX, USA, "Tutorial – Using a Desktop Computer as a LabVIEW Real-Time for ETS Target", August 2007.

[7] National Instruments Inc, Austin, TX, USA, "Tutorial – LabVIEW FPGA 8 Module Training", February 2006.

[8] L. Burian, P. Fuchs, "A simple active noise control in acoustic duct," IEEE Conference on Circuit Theory and Design, Volume 3, 2005.